ACS OMEGA

http://pubs.acs.org/journal/acsodf

Article

Suppression of Esophageal Squamous Cell Carcinoma Development by Mechanosensitive Protein Piezo1 Downregulation

Lu Gao, Yun Ji, Lulu Wang, Meixia He, Xiaojing Yang, Yibing Qiu, Xu Sun, Zhenyu Ji, Guanrui Yang, Jianying Zhang, Shanshan Li, Liping Dai,* and Liguo Zhang*

Cite This: *ACS Omega* 2021, 6, 10196−10206

Read Online

ACCESS | Metrics & More | Article Recommendations | Supporting Information

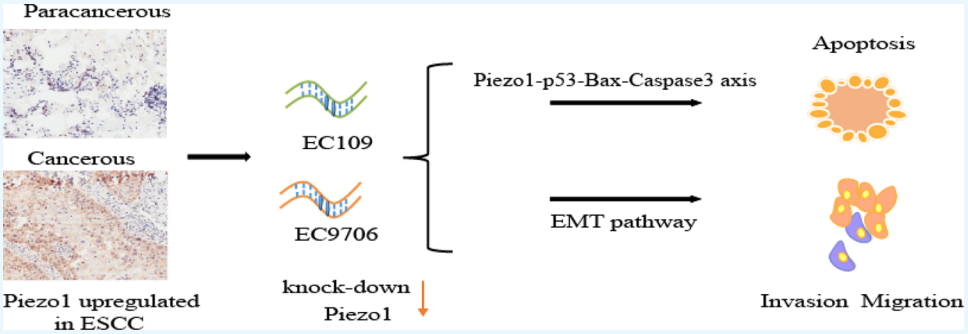

ABSTRACT: Esophageal squamous cell carcinoma (ESCC) is a malignant epithelial cancer of the esophageal epithelium. Piezo-type mechanosensitive ion channel component 1 (Piezo1), an essential mechanosensitive protein, plays an important role in maintaining cell biological functions under the stimulation of physiological force. Immunohistochemical and bioinformatic analyses of ESCC tissue samples indicate that Piezo1 expression is higher in ESCC tissues than in paracancerous tissues. shRNA-mediated Piezo1 downregulation in the ESCC lines EC9706 and EC109 showed that proliferation, migration, and invasion were suppressed by Piezo1 knockdown. Piezo1 downregulation suppresses ESCC migration and invasion in both cells and tissues via the epithelial−mesenchymal transition pathway. Moreover, G0/G1 to S-phase cell cycle progression was inhibited, and cell apoptosis was induced by Piezo1 downregulation. Furthermore, we observed an interaction between Piezo1 and p53 using immunoprecipitation. The protein levels of p53, downstream factor Bax, apoptosis executioner cleaved-caspase3, and caspase3 were significantly upregulated by the downregulation of Piezo1. The inhibited growth rate and upregulated expression of these related factors were validated using tumor-bearing mice. Therefore, Piezo1 downregulation induces ESCC apoptosis via a Piezo1−p53−Bax−Caspase 3 axis. In conclusion, Piezo1 downregulation suppresses ESCC development, and mechanosensitive protein Piezo1 can be considered a new target for ESCC therapy.

1. INTRODUCTION

Esophageal squamous cell carcinoma (ESCC) is a malignant epithelial cancer of the esophageal epithelium.[31] It has a poor prognosis, with an overall 5-year survival rate of <20% after diagnosis.[9,11] As the swallowing organ, the esophageal epithelium is continuously stimulated by the passage of food. Epidemiological studies have demonstrated that dietary habits, such as swallowing roughage-containing food without sufficient mastication[10,16] or consuming hot drinks[17] and spicy food,[27] are possible predisposing etiologic factors for ESCC. In addition, physical damage[25] or force[33] in the tumor microenvironment is believed to induce ESCC.[26] These ESCC factors are associated with mechanical stimulation. At the cellular level, cells sense mechanical forces through mechanoreceptors and respond by modifying their behavior and microenvironment.[2] Yu et al. reviewed the effects of biomechanical regulation at the molecular, cellular, and tissue levels and confirmed that the regulation influences cancer occurrence and progression.[36]

Piezo-type mechanosensitive ion channel component 1 (Piezo1) is a mechanosensitive channel in mammals.[7] It senses and transduces mechanical stimulation to regulate physical sensations, such as pain and touch.[19] Under various external mechanical stimuli, Piezo1 functions as a mechanical sensor to influence cell generation, proliferation, differentiation, and survival by regulating intracellular calcium ion levels.[15,23,38] In cancer research, Piezo1 has been shown to promote the migration and invasion of melanoma,[15] osteosarcoma,[18] breast cancer,[20] and glioma cells.[5] In gastric cancer, Piezo1 promotes

Received: January 27, 2021
Accepted: March 31, 2021
Published: April 12, 2021

cell migration and invasion by interacting with the trefoil factor family.[37] In addition, Piezo1 influences prostate cancer development by activating the Akt/mTOR pathway and enhancing cell cycle progression.[13] These studies confirmed that Piezo1 protein plays an important role in cancer occurrence and progression. However, few studies have reported the role of Piezo1 in ESCC.

Piezo1 is relatively highly expressed in the esophagus than other human tissues.[35] In normal epithelial cells, Piezo1 is the primary factor that senses mechanical stimulation to control cell behavior and is considered a critical protein for tumor development.[8,12] ESCC development involves a significantly increased tumor volume, which induces esophageal stenosis and increases stress.[32] These mechanical forces stimulate the esophageal endothelial cells.[25] Moreover, Piezo1 in ESCC cells may be stimulated, leading to ESCC development. Therefore, it is useful to investigate the role of Piezo1 in ESCC. The expression of the underlying Piezo1 was investigated using clinical samples and ESCC cell lines, the effect and mechanism of Piezo1 downregulation on ESCC cells' biological function were explored, and the results were validated in tumor-bearing mice.

2. RESULTS AND DISCUSSION

2.1. Piezo1 Expression in Esophageal Tissues. The protein expression of Piezo1 was evaluated by immunohistochemical staining. As shown in Table 1, 53.06 and 26.53% of the ESCC samples showed moderate and strong Piezo1 expressions, respectively. By contrast, only 24% of the paracancerous samples exhibited moderate Piezo1 expression, and no paracancerous sample showed positive Piezo1 expression. The number of ESCC samples that showed either weak or negative Piezo1 expression was smaller than that of paracancerous tissues showing either weak or negative Piezo1 expression. Hence, the protein expression of Piezo1 was evidently higher in ESCC tissues than in paracancerous tissues. The immunohistochemical staining image of the paracancerous and ESCC samples in stage IV is shown in Figure 1a.

Table 1. Piezo1 Expression in Cancerous and Paracancerous Tissues

	tumor		normal		
group rank	count	%	count	%	*p*-value
−	4	8.16	7	28	
+	6	12.24	12	48	
++	26	53.06	6	24	<0.001
+++	13	26.53	0	0	
total	49	100	25	100	

Piezo1 gene expression in 81 ESCC and 11 normal samples from the TCGA database was analyzed using R to verify the experimental results. Piezo1 gene expression levels in the ESCC samples were significantly higher than those in the normal samples (Figure 1b), which was consistent with the immunohistochemical results. Therefore, Piezo1 expression at both the protein and gene levels was higher in ESCC tissues than in paracancerous tissues.

2.2. Piezo1 Downregulation in ESCC Cell Lines. The Piezo1 mRNA expression level in five human ESCC cell lines (EC109, EC9706, TE-1, KYSE510, and KYSE30) was first examined to generate Piezo1-downregulated cells. As shown in Figure 2a, EC109 and EC9706 cell lines showed higher Piezo1 expression levels than the other three cell lines. shRNA-Piezo1 was therefore transfected into EC109 and EC9706 cells to obtain stably transfected cell lines. The Piezo1-silencing efficiency in transfected EC109 and EC9706 cells was significant at the protein level (Figure 2b). Furthermore, the relative mRNA expression of Piezo1 in EC109 and EC9706 cells transfected using shRNA-Piezo1 was significantly downregulated compared with those transfected using the shRNA-control (Figure 2c,d). These results confirmed the successful generation of Piezo1-downregulated cells and the corresponding control cell lines $EC109^{shRNA\text{-}piezo1}$, $EC109^{shRNA\text{-}control}$, $EC9706^{shRNA\text{-}piezo1}$, and $EC9706^{shRNA\text{-}control}$.

2.3. Piezo1 Downregulation Inhibits the Increase in the Intracellular Ca^{2+} Level. Piezo1 is a selective calcium ion channel that can be activated by Piezo1 agonist Yoda1.[6] The fluorescence intensity (FI) of intracellular Ca^{2+} observed before the addition of Piezo1 agonist Yoda1 is shown in Figure 3a,b. Intracellular Ca^{2+} in $EC109^{shRNA\text{-}piezo1}$ and $EC9706^{shRNA\text{-}piezol}$ was lower than that in $EC109^{shRNA\text{-}control}$ and $EC9706^{shRNA\text{-}control}$. The increase in the intracellular Ca^{2+} level by the addition of Yoda1 was calculated, and the increase in the intracellular Ca^{2+} level after the addition of Yoda1 into $EC9706^{shRNA\text{-}piezo1}$ and $EC109^{shRNA\text{-}piezo1}$ cells was lower than that in $EC9706^{shRNA\text{-}control}$ and $EC109^{shRNA\text{-}control}$ cells (Figure 3c,d). Hence, Piezo1 downregulation in the proven cell lines suppresses the increase in the intracellular Ca^{2+} level, reconfirming that stable $EC109^{shRNA\text{-}piezo1}$, $EC109^{shRNA\text{-}control}$, $EC9706^{shRNA\text{-}piezo1}$, and $EC9706^{shRNA\text{-}control}$ cell lines were successfully established.

2.4. Piezo1 Downregulation Inhibits ESCC Cell Migsration and Invasion via the Epithelial−Mesenchymal Transition (EMT) Pathway. The migration and invasion of transfected EC109 cells were measured using wound-healing and transwell chamber assays, respectively. The migration and invasion of $EC109^{shRNA\text{-}piezo1}$ cells were both remarkably inhibited by the downregulation of Piezo1 (Figure 4a−c). The migration and invasion of $EC9706^{shRNA\text{-}piezo1}$ cells were also examined using transwell chamber assays. The migration and invasion of $EC9706^{shRNA\text{-}piezo1}$ cells were similarly both suppressed by the downregulation of Piezo1 (Figure 4d,e). The mechanism underlying the effects of Piezo1 on the migration and invasion of ESCC cells was assessed by evaluating the expression of E-cadherin and N-cadherin in the EMT pathway. The expression of E-cadherin was upregulated in $EC109^{shRNA\text{-}piezo1}$ and $EC9706^{shRNA\text{-}piezo1}$ cells, and the expression of N-cadherin was decreased in $EC109^{shRNA\text{-}piezo1}$ and $EC9706^{shRNA\text{-}piezo1}$ cells (Figure 4f). Thus, the downregulation of Piezo1 inhibited the migration and invasion of ESCC cells via the EMT pathway.

2.5. Piezo1 Downregulation Impairs Cell Growth and Induces the Apoptosis of ESCC Cells. Because the migration and invasion of both $EC109^{shRNA\text{-}piezo1}$ and $EC9706^{shRNA\text{-}piezo1}$ cells were inhibited by the downregulation of Piezo1, the proliferation, cell cycle progression, and apoptosis of transfected EC109 and EC9706 cells were examined using the cell counting kit-8 (CCK-8) assay, flow cytometry, and terminal deoxynucleotidyl transferase dUTP nick end labeling (TUNEL) assay. The proliferation of transfected EC109 and EC9706 cells is shown in Figure 5a,b. The proliferation of $EC109^{shRNA\text{-}piezo1}$ cells was inhibited by 50% following the downregulation of Piezo1 compared with that of $EC109^{shRNA\text{-}control}$ cells. Likewise, the proliferation of $EC9706^{shRNA\text{-}piezo1}$ cells was decreased by 30% after the downregulation of Piezo1 compared with that of $EC9706^{shRNA\text{-}control}$ cells. Furthermore, the numbers of S-phase

https://doi.org/10.1021/acsomega.1c00505
ACS Omega 2021, 6, 10196−10206

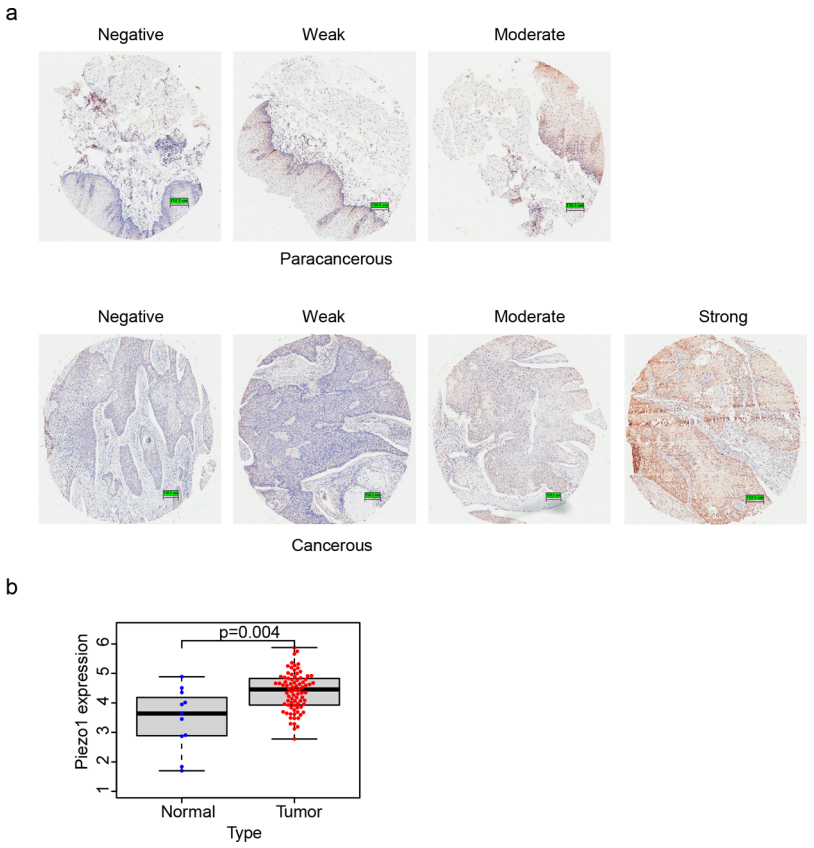

Figure 1. Piezo1 expression in tissues. (a) Immunohistochemical images of Piezo1 expression in paracancerous tissues (above) and ESCC tissues (below). (b) Relative expression level of Piezo1 in the cancer genome atlas (TCGA) samples.

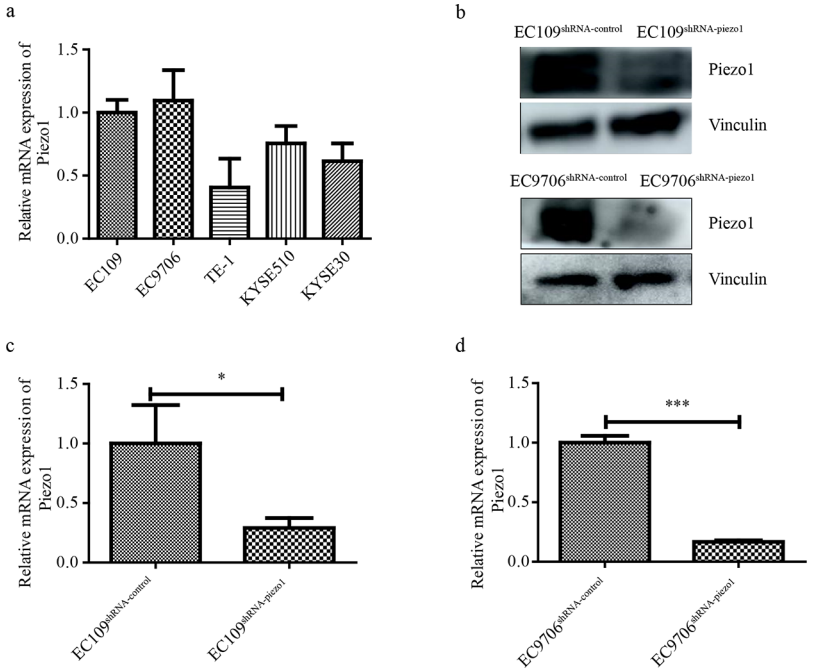

Figure 2. Construction of Piezo1-downregulated cell lines. (a) Piezo1 mRNA expression in different ESCC cell lines. (b) Protein expression of Piezo1 in transfected EC9706 and EC109 cell lines. (c and d) Relative mRNA expression of Piezo1 in transfected EC9706 and EC109 cell lines. * $p < 0.05$ vs control and *** $p < 0.001$ vs control.

$EC109^{shRNA\text{-}piezo1}$ and $EC9706^{shRNA\text{-}piezo1}$ cells were reduced by the downregulation of Piezo1 (Figure 5c–f). The downregulation of Piezo1 also induced the apoptosis of $EC109^{shRNA\text{-}piezo1}$ and $EC9706^{shRNA\text{-}piezo1}$ cells (Figure 5g–h). The expression of apoptotic factors, caspase3, and cleaved-caspase3 in $EC109^{shRNA\text{-}piezo1}$ and $EC9706^{shRNA\text{-}piezo1}$ cells at the

https://doi.org/10.1021/acsomega.1c00505
ACS Omega 2021, 6, 10196−10206

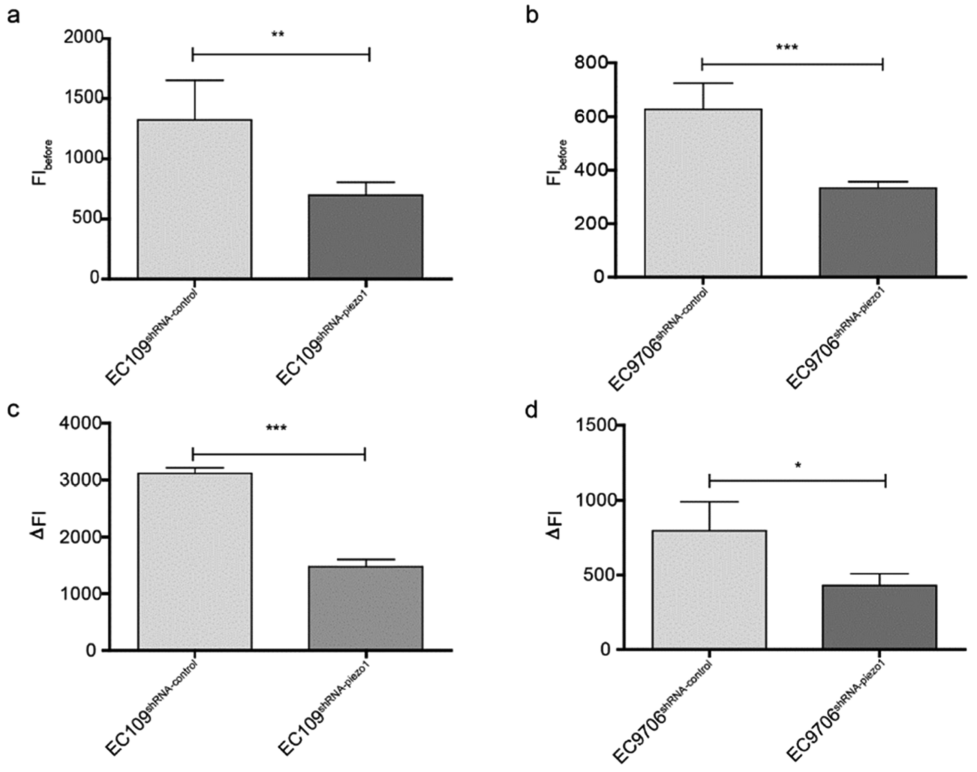

Figure 3. FI of intracellular Ca^{2+} and intracellular Ca^{2+} levels increased by Yoda1. (a) FI_{before} in $EC109^{shRNA\text{-}piezo1}$ and $EC109^{shRNA\text{-}control}$ cells. ** $p <$ 0.001 vs control. (b) FI_{before} in $EC9706^{shRNA\text{-}piezo1}$ and $EC9706^{shRNA\text{-}control}$ cells. *** $p < 0.001$ vs control. (c) ΔFI in $EC109^{shRNA\text{-}piezo1}$ and $EC109^{shRNA\text{-}control}$ cells. *** $p < 0.05$ vs control. (d) ΔFI in $EC9706^{shRNA\text{-}piezo1}$ and $EC9706^{shRNA\text{-}control}$ cells. * $p < 0.05$ vs control.

protein level was significantly higher than that in $EC109^{shRNA\text{-}control}$ and $EC9706^{shRNA\text{-}control}$ cells (Figure 5i). These results indicate that the downregulation of Piezo1 suppressed the proliferation and promoted the apoptosis of ESCC cells.

2.6. Piezo1 Interacts with p53 to Regulate the p53/Bax Pathway. The p53 pathway plays important roles in cell cycle arrest and apoptosis.[4] The possible relationship between Piezo1 and p53 was evaluated to determine the molecular mechanism underlying Piezo1 in ESCC development using co-immunoprecipitation (co-IP). The expression of p53 was found in proteins adsorbed by Piezo1 antibody in both EC109 and EC9706 cells (Figure 6a). Hence, Piezo1 is capable of interacting with p53. Bax is a critical protein in the downstream of the p53 pathway. The expressions of p53 and Bax in transfected EC109 and EC9706 cells at both the gene and protein levels were significantly higher in $EC109^{shRNA\text{-}piezo1}$ and $EC9706^{shRNA\text{-}piezo1}$ cells than in $EC109^{shRNA\text{-}control}$ and $EC9706^{shRNA\text{-}control}$ cells (Figure 6b,c). Therefore, Piezo1 interacts with p53 and regulates the expression of Bax in the downstream of the p53 pathway, which affects ESCC apoptosis.

To verify the interaction between p53 and Piezo1, a rescue experiment was performed. The expression of p53 was inhibited using a p53 inhibitor, and the expression of Piezo1 was measured. As shown in Figure 6d,e, p53 inhibition induced Piezo1 upregulation in both EC9706 and EC109 cells. This reconfirmed that p53 and Piezo1 interact with each other.

2.7. Tumor Growth Is Inhibited In Vivo by Piezo1 Downregulation. Transfected EC109 cells were injected into the subcutaneous tissues of BALB/c nude mice named $mice^{shRNA\text{-}piezo1}$ and $mice^{shRNA\text{-}control}$. The results showed that after 23 days, the tumor sizes in $mice^{shRNA\text{-}piezo1}$ were evidently smaller than those in $mice^{shRNA\text{-}control}$ (Figure 7a). Moreover, at the end of the experiment, the tumor weights of $mice^{shRNA\text{-}piezo1}$ were lower than those of $mice^{shRNA\text{-}control}$ (Figure 7b). Furthermore, the tumor volume was recorded every 2 days, and the results indicated that tumors in $mice^{shRNA\text{-}piezo1}$ showed a slower growth rate than those in $mice^{shRNA\text{-}control}$ (Figure 7c).

Similar to the in vitro experiments, protein expression levels of factors related to migration, invasion, and apoptosis were affected by the downregulation of Piezo1 in vivo. With respect to factors associated with migration and invasion, the protein expression level of E-cadherin was upregulated and that of N-cadherin was downregulated in the tumor tissues harvested from $mice^{shRNA\text{-}piezo1}$ compared with those in the tumor tissues from $mice^{shRNA\text{-}control}$; alternatively, factors related to apoptosis and protein levels of p53, cleaved-caspase3, caspase3, and Bax were upregulated in the tumor tissues harvested from $mice^{shRNA\text{-}piezo1}$ compared with those in the tumor tissues from $mice^{shRNA\text{-}control}$ (Figure 7d).

3. DISCUSSION

Cell migration and invasion are complex processes that can lead to tumor formation and progression. In colon cancer, Piezo1 promotes cell migration and invasion via a possible regulatory mechanism involving the Piezo1−MCU−HIF-1α−VEGF axis.[28] In other cancers, such as melanoma,[15] prostate cancer,[13] osteosarcoma,[18] breast cancer,[20] glioma,[5] and human synovial sarcoma,[29] Piezo1 has been shown to promote cell metastasis and invasion. In our study, Piezo1 downregulation inhibited ESCC migration and invasion. EMT is a process that converts epithelial cells into mesenchymal cells and is frequently activated during cancer migration and invasion.[30] It has been reported that some genes, such as WISP2, exhibit their potential

https://doi.org/10.1021/acsomega.1c00505
ACS Omega 2021, 6, 10196−10206

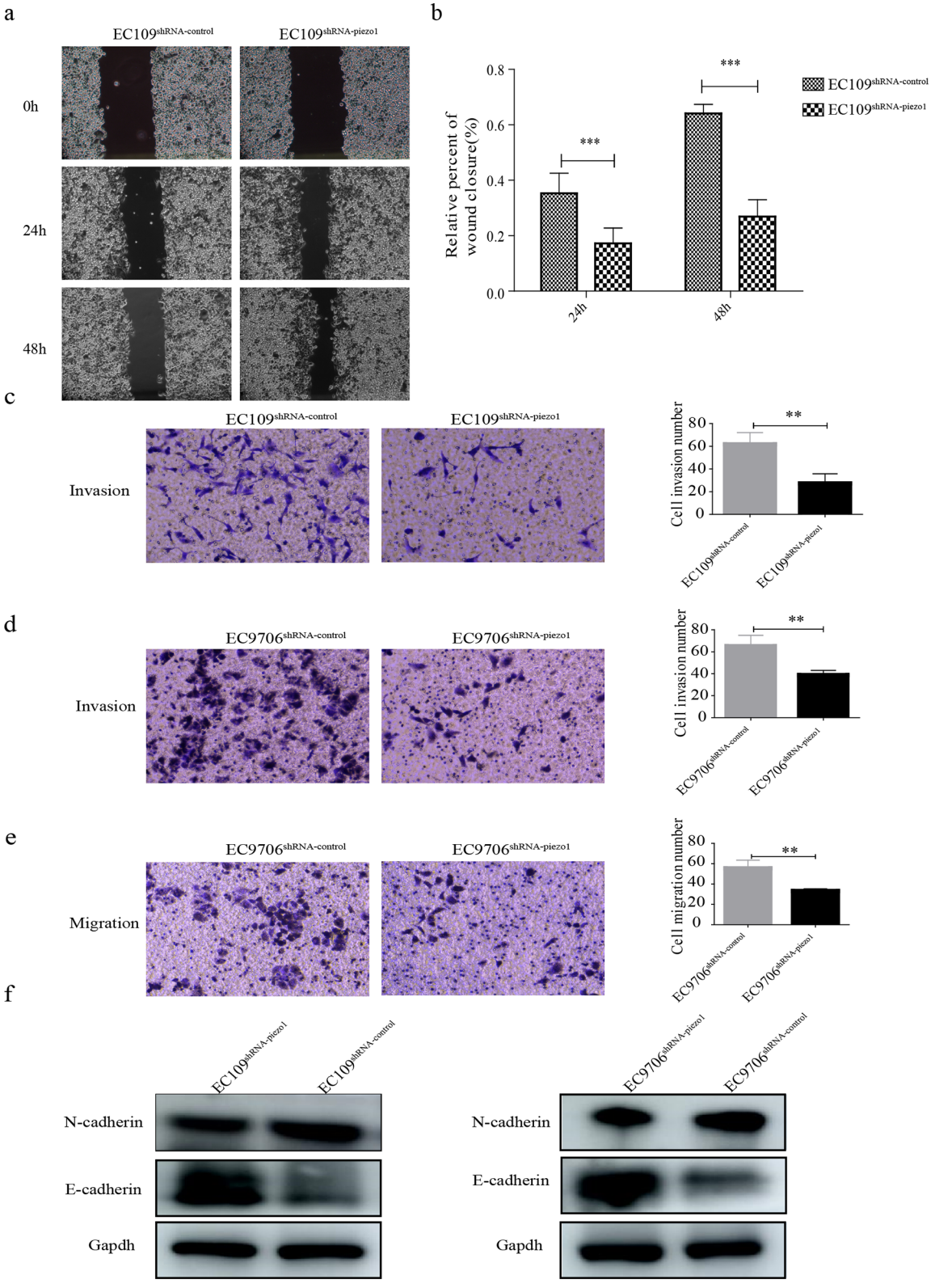

Figure 4. Migration and invasion of transfected cells. (a) Migration of EC109$^{shRNA\text{-}piezo1}$ and EC109$^{shRNA\text{-}control}$ cells. (b) Quantitative analysis of panel A, *** $p < 0.001$ vs control. (c) Invasion of EC109$^{shRNA\text{-}piezo1}$ and EC109$^{shRNA\text{-}control}$ cells, ** $p < 0.01$ vs control. (d and e) Invasion and migration of EC9706$^{shRNA\text{-}piezo1}$ and EC9706$^{shRNA\text{-}control}$ cells, ** $p < 0.01$ vs control. (f) Protein expression of E-cadherin and N-cadherin in transfected EC109 and EC9706 cells.

antitumor activity by targeting the E-cadherin pathway in ESCC.[3] In our study, we found that downregulating Piezo1 increased the E-cadherin level and decreased the N-cadherin level in both cells and tissues. Thus, the downregulation of Piezo1 may inhibit the invasion and migration of ESCC cells via the EMT pathway.

https://doi.org/10.1021/acsomega.1c00505
ACS Omega 2021, 6, 10196−10206

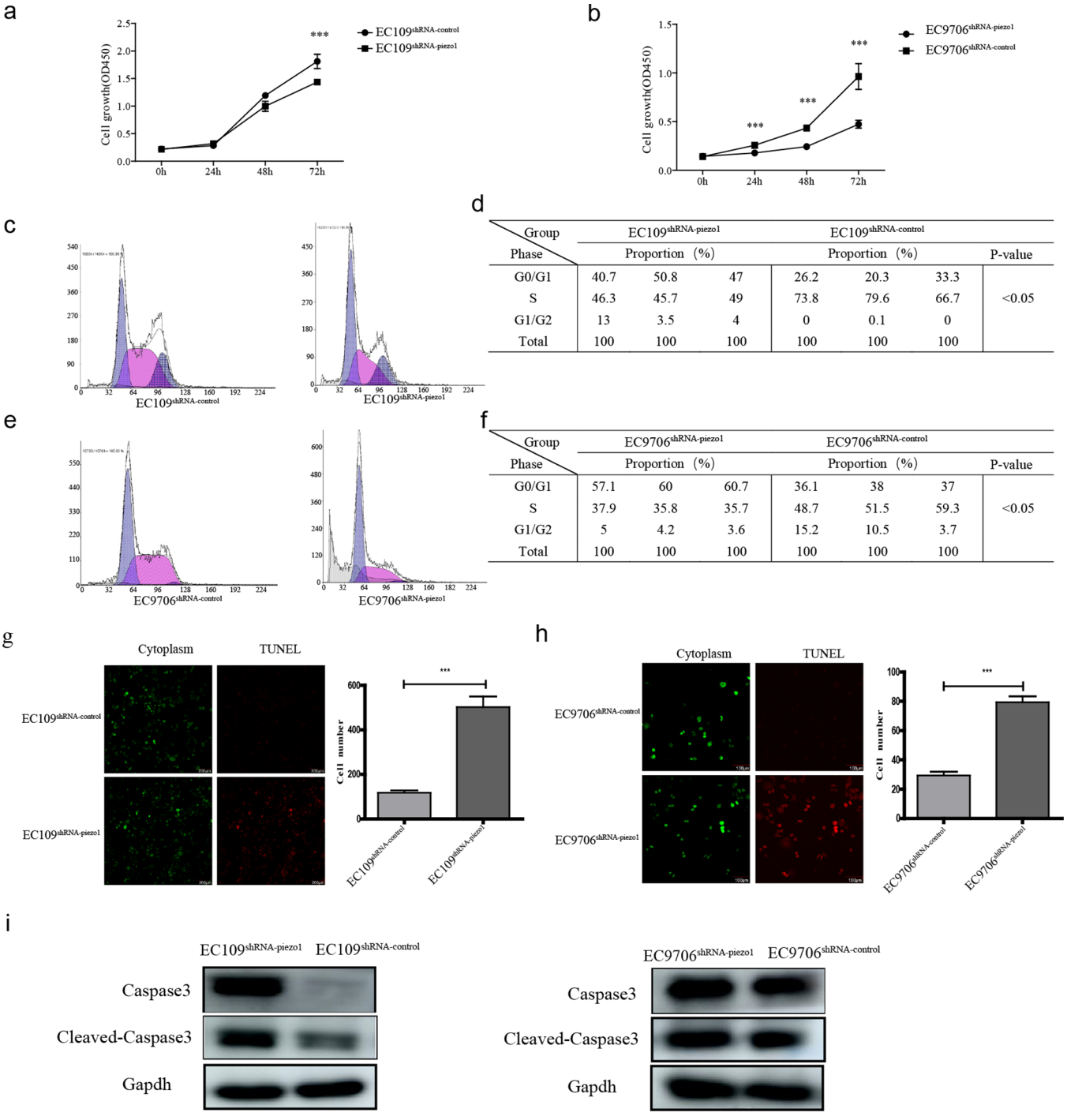

Figure 5. Piezo1 downregulation affects ESCC cell proliferation, cell cycle progression, and apoptosis. Proliferation was suppressed by Piezo1 downregulation in (a) EC109 cells and (b) EC9706 cells, *** $p < 0.001$ vs control. (c) Cell cycle distribution of transfected EC109 cells. (d) Analysis of cell cycle distribution in panel C, * $p < 0.05$ vs control. (e) Cell cycle distribution of transfected EC109 cells. (f) Analysis of cell cycle distribution in panel E, * $p < 0.05$ vs control. Apoptosis of transfected (g) EC109 cells and (h) EC109 cells. (i) Protein expressions of cleaved-caspase3 and caspase3 in transfected EC109 and EC9706 cells, respectively.

Under stress conditions, such as in tumor microenvironments, p53 is considered a critical cellular stress sensor that induces cell cycle arrest, cellular senescence, apoptosis, DNA repair, or autophagy.[1] In ESCC, LincRNA-p21 was found to regulate ESCC cell apoptosis by modulating the p53 pathway,[39] but only a few reports have confirmed the correlation between Piezo1 and p53. In this study, Piezo1 was shown to interact with p53, regulating the expression of downstream factors in the p53 pathway leading to the apoptosis of ESCC. Several downstream pathways are associated with p53.[14] The p53/Bax mitochondrial apoptosis pathway is primarily regulated via the p53 effector Bax, which is located in the outer membrane of the mitochondria.[34] Caspase3 is a crucial executioner of apoptosis and is activated to cleaved-caspase3 in apoptotic cells.[24] Downregulated Piezo1 protein in the present study upregulated the expressions of p53 protein, downstream factor Bax, and apoptosis executioner cleaved-caspase 3. This finding was validated at both the cell and tissue levels. Thus, the downregulation of Piezo1 promotes the

https://doi.org/10.1021/acsomega.1c00505
ACS Omega 2021, 6, 10196−10206

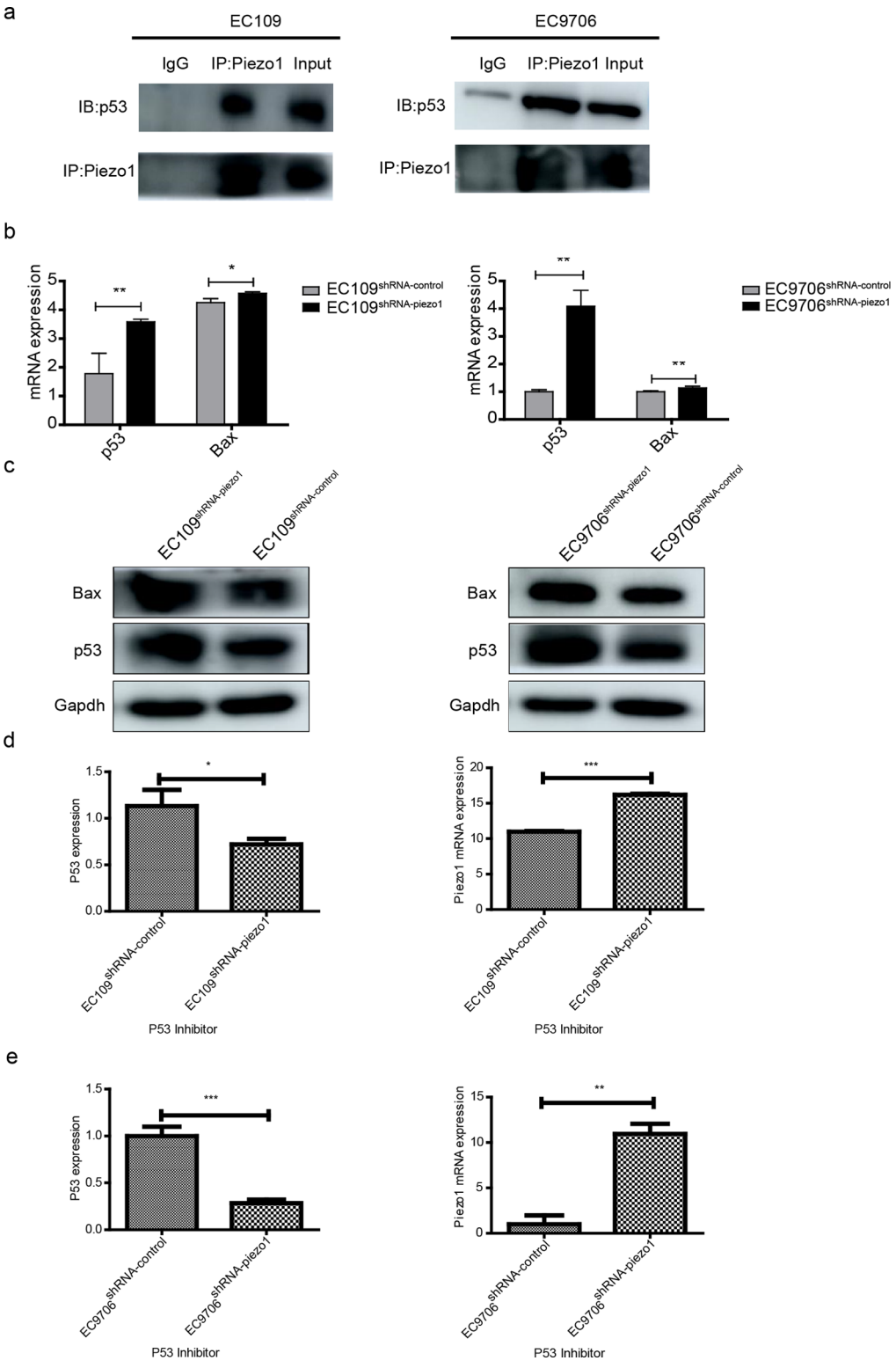

Figure 6. Interaction between p53 and Piezo1, and the protein expression of p53 and Bax. (a) Co-IP between Piezo1 and p53 in EC109 and EC9706 cells. Cell lysates underwent IP using control IgG or the indicated antibody, and the precipitated protein was detected using immunoblotting analysis with the indicated antibody. Cell extracts were used as a positive control (input). (b) Relative mRNA levels of p53 and Bax in transfected EC109 and EC9706 cells, respectively. ** $p < 0.01$ vs control and * $p < 0.05$ vs control. (c) Protein expressions of p53 and Bax in transfected EC109 and EC9706 cells, respectively. (d) Relative mRNA expression levels of Piezo1 and p53 in EC109 and (e) EC9706 cell lines after the addition of the p53 inhibitor.

activation of p53 and induces the apoptosis of ESCC cells by a Piezo1−p53−Bax−Caspase 3 axis (Figure 8).

Cell proliferation and cell cycle progression are generally considered to be closely related to cell apoptosis.[34] The p53 pathway is also a classical apoptosis pathway. As a downstream factor of the p53 pathway, Bax has been targeted for cell cycle arrest and cell death.[21] In our study, the increased expression of Bax induced by the downregulation of Piezo1 also inhibited cell

https://doi.org/10.1021/acsomega.1c00505
ACS Omega 2021, 6, 10196−10206

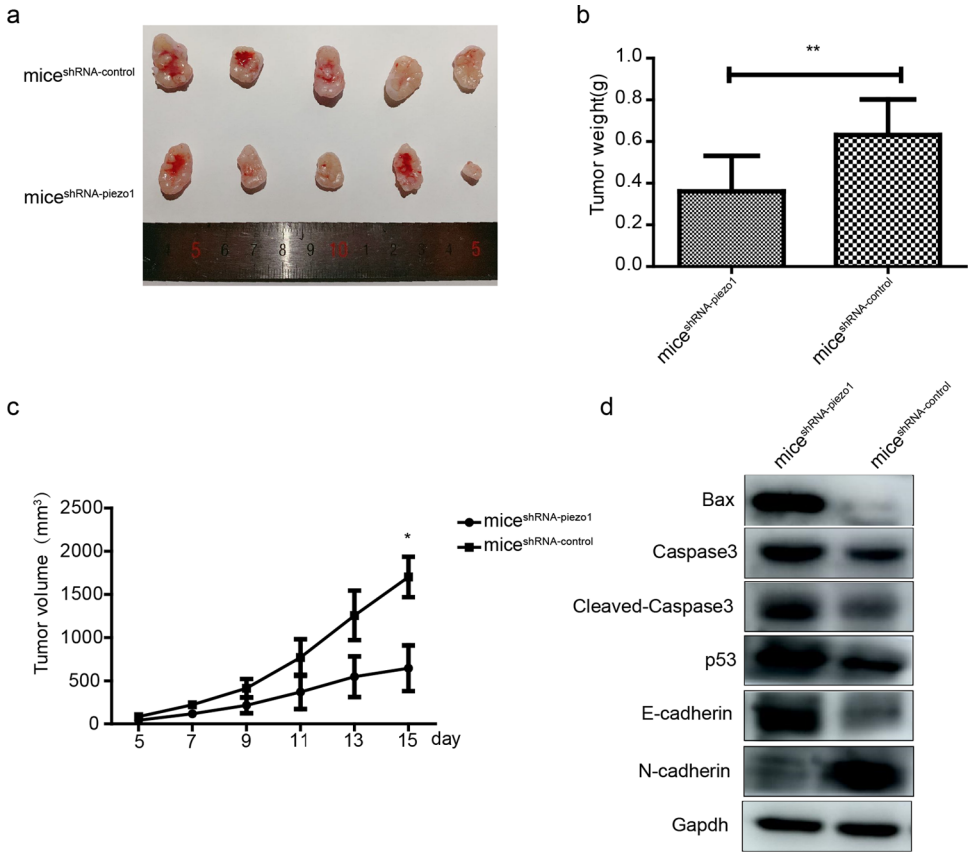

Figure 7. Tumor growth in tumor-bearing mice. (a) Images of tumors harvested from mice$^{shRNA\text{-}piezo1}$ and mice$^{shRNA\text{-}control}$. (b) Final weights of tumors in mice$^{shRNA\text{-}piezo}$ and mice$^{shRNA\text{-}control}$. $^{**}p < 0.01$ vs control. (c) Tumor volumes measured throughout the experiment. $^{*}p < 0.05$ vs control. (d) Protein expression of Bax, cleaved-caspase3, caspase3, p53, E-cadherin, and N-cadherin in tumor tissues.

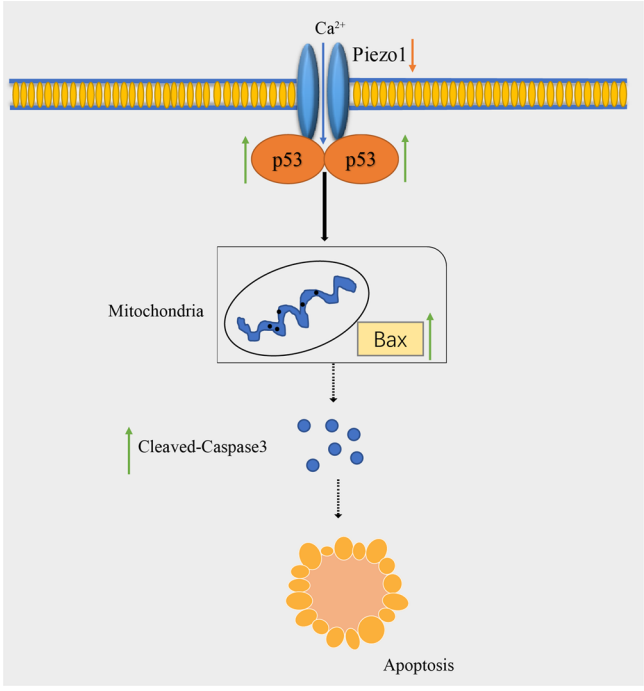

Figure 8. Schema of the Piezo1-p53-Bax-Caspase 3 axis.

proliferation and blocked the cell cycle. Therefore, the decreased proliferation and blocked cell cycle were at least partly responsible for the increased apoptosis. In addition, Piezo1 as an oncogene has been reported to play an important role in modulating gastric cancer cell proliferation,[37] osteosarcoma proliferation,[18] and the prostate cancer cell cycle.[13] Our results are consistent with these studies.

Piezo1 senses and conducts mechanical stimulation in esophageal epithelial cells. In the human esophagus, long-term stimulation by swallowing roughage-containing food induces the continuous activation of Piezo1. Mechanical stimuli during ESCC development could also act as a possible stimulus to activate Piezo1 and influence ESCC development. As a crucial mechanical sensitive protein, Piezo1 is highly expressed in ESCC tissue. Its downregulation suppresses ESCC cell invasion and migration via the EMT pathway and promotes ESCC cell apoptosis via the Piezo1−p53−Bax−Caspase 3 axis. Therefore, Piezo1 downregulation could suppress ESCC development, and the mechanosensitive protein Piezo1 could be a new target for ESCC therapy.

4. MATERIALS AND METHODS

4.1. Cell Culture. Human ESCC cell lines (EC109, EC9706, TE-1, KYSE30, and KYSE510) were purchased from the Chinese National Infrastructure of Cell Line Resource and cultured in RPMI 1640 (Solaibao, China) supplemented with 10% fetal bovine serum (BI, USA). All cells were incubated at 37 °C with 5% CO_2.

4.2. Bioinformatic Analysis of TCGA Data. TCGA gene expression data for ESCC, including 81 cancer samples and 11 normal samples, were retrieved from XENA (http://xena.ucsc.edu/) to verify Piezo1 expression in ESCC tissues using

https://doi.org/10.1021/acsomega.1c00505
ACS Omega 2021, 6, 10196−10206

Student's *t*-test. The expression was converted using log2. Limma packages were used for performing differential analysis between 81 ESCC and 11 normal samples.

4.3. Immunohistochemical Analysis of Tissue Samples. Seventy-four tissue samples, including 49 ESCC and 25 paracancerous tissues with their corresponding pathological information, were provided by Shanghai Xinchao Biotechnology Co., Ltd. (China). The samples were incubated with an anti-Piezo1 antibody (diluted 1:1000) at 4 °C overnight (Abcam, UK) and IgG-HRP secondary antibody (Shanghai Universal Biotech Co., Ltd. China). Immunofluorescence images were obtained using a digital pathology scanner (AperioCS2, Leica, Germany). The protein expression level of Piezo1 was categorized into the following four groups based on the immunostaining intensity: negative (−: score 0), weak (+: score 0.5), moderate (++: score 1), and strong (+++: score 2).

4.4. Plasmid Construction and Transfection. shRNA (GCCTCGTGGTCTACAAGAT) carrying the human Piezo1 gene (shRNA-Piezo1) and control shRNA (TTCTCCGAACGTGTCACGT) lentiviruses (shRNA-control) were generated by HeYuan Biotechnology Co., Shanghai, China. We used a lentiviral vector (pLKD-CMV-G&PR-U6-shRNA) containing an enhanced green fluorescent protein and puromycin-resistant gene. Two ESCC cell lines (EC109 and EC9706) were used to construct stably transfected cell lines. They were then seeded into 24-well plates (10^5 cells/well) and infected with shRNA lentiviruses using polybrene. Puromycin (1 μg/mL, Solaibao, China) was used to screen stably infected cells. Stably transfected cell lines were named as follows: EC109shRNA-Piezo1, EC109shRNA-control, EC9706 shRNA-Piezo1, and EC9706 shRNA-control. The cells were treated with 10 μM p53 inhibitor and Pifithrin-α (Selleck, USA) for 48 h, and total RNA was extracted.

4.5. Quantitative Reverse Transcription-Polymerase Chain Reaction (qRT-PCR). The total RNA from cells was isolated using Trizol (Solaibao, China) and reverse-transcribed into cDNA using a reverse transcription system (Takara, Japan). qRT-PCR was performed using a real-time PCR system (Roche, Germany). SYBR Green (Takara, Japan) was used as a fluorescent dye. Transcripts were quantified using glyceraldehyde 3-phosphate dehydrogenase as an internal standard. All primer sequences (Sangon Inc., China) are listed in S1.

4.6. Detection of Intracellular Ca^{2+} Increased by the Stimulation of Yoda1. Transfected EC109 and EC9706 cells were seeded into laser confocal dishes (20 mm in diameter and 10^5 cells/dish). After incubation for 24 h for cell adhesion, 500 μL of the calcium probe (3 μM, Rhod 2-AM, Thermo Fisher, USA) was added to each dish and incubated at 37 °C in the dark for 40 min. Cells were rinsed twice with phosphate-buffered saline (PBS) and then incubated in 1 mL of Hank's solution (Solaibao, China) for 30 min. The FI of intracellular Ca^{2+} was detected using laser scanning confocal microscopy (LSCM; Olympus, Japan) with an excitation wavelength of 557 nm. Then, 1 mL of Piezo1 agonist Yoda1 (26.6 μM, Glpbio, USA) was added, and cells were incubated for 10 min. The FI of intracellular Ca^{2+} was detected using LSCM with the same image acquisition parameters. For every measurement, three duplicate samples were used in the experiment. For every image, the average FI of 10 cells was defined as the FI of intracellular Ca^{2+}. The FI of intracellular Ca^{2+} detected before the addition of Yoda1 was denoted as FI_{before}, and the FI of intracellular Ca^{2+} detected after the addition of Yoda1 was denoted as FI_{after}. The increase in intracellular Ca^{2+} after the stimulation of Yoda1 was calculated using the following formula: $\Delta FI = FI_{after} - FI_{before}$.

4.7. TUNEL Assay. After collection, cells were fixed with 4% paraformaldehyde (Solaibao, China) and then rinsed with PBS thrice. The remaining procedure for the TUNEL assay was performed as per the manufacturer's instructions (Meilunbio, China). Cells were incubated with proteinase K (20 μg/mL in PBS) for 5 min at ambient temperature and then dyed using 0.5% crystal violet staining solution. Fluorescent images were obtained using LSCM.

4.8. Cell Viability Assay. Transfected cells were seeded into 96-well plates (5000 cells/well), and cell viability was determined using the CCK-8 assay (Meilunbio, China) following the manufacturer's instructions. Optical density (OD450) was measured using a microplate reader (Bio-Rad, USA).

4.9. Wound-Healing Assay. The migration of transfected EC109 cells was evaluated using wound-healing assays. Once the transfected cells reached 95% confluence in six-well plates, the cell monolayer was scratched using a 200 μL pipette tip, and the cells were washed thrice with PBS. The cells were cultured in a serum-free culture medium, and images were acquired at 0, 24, and 48 h postscratching.

4.10. Transwell Invasion and Migration Assay. Invasion assays were performed for both transfected EC109 and EC9706 using transwell chambers (Corning, USA) with a thin coating of Matrigel (BD Biosciences, USA). The diluted (1,9, 5×10^5) cells were seeded in the upper chamber containing a serum-free culture medium, and the bottom chamber was filled with 600 μL of medium containing 20% fetal bovine serum (BI, USA). After 72 h incubation, cells in the chambers were fixed and stained using crystal violet (Solaibao, China). Images of invading cells were captured using a microscope.

Transfected EC9706 cells were then seeded in the upper chamber at 2×10^5 cells/chamber to assess their migration. After 48 h incubation, cells in the lower chamber were washed, fixed, and stained using crystal violet. Next, invading cells were counted, and cell images were captured using a microscope.

4.11. Cell Cycle Analyses via Flow Cytometry. After collection, the cells were fixed with 75% ethanol at 4 °C overnight, rinsed twice with PBS, and centrifuged. Then, the cells were incubated in 50 μg/mL propidium iodide dye (Solaibao, China) for 1 h. Finally, a flow cytometer (Beckman, USA) was used for detecting the cell cycle phases.

4.12. Western Blotting. Cells and mouse tissue ground in liquid nitrogen were lysed in radioimmunoprecipitation assay buffer (Meilunbio, China) to obtain protein lysates. Total proteins were collected from the supernatant after centrifugation, and the proteins were quantified using the bicinchoninic acid (Thermo Fisher, USA) assay. Equal amounts of protein were separated using sodium dodecyl sulfate-polyacrylamide gel electrophoresis and transferred onto polyvinylidene fluoride membranes. The membranes were blocked with 5% milk powder in tris-buffered saline with Tween 20 for 2 h at ambient temperature and then incubated with primary antibodies at 4 °C overnight. After washing, the membranes were incubated with secondary antibodies for 2 h at ambient temperature. Proteins on the membrane were visualized using a chemiluminescence kit (Thermo Fisher, USA).[22] All other primary antibodies and their dilutions are listed in S2.

During the acquisition of western blotting images, it was found that the marker always showed a heavy stripe following the addition of the developing solution, and the brightness of the

https://doi.org/10.1021/acsomega.1c00505
ACS Omega 2021, 6, 10196−10206

nearby stripe was significantly altered during the exposure process. Therefore, the marker in some of the western blot bands was cut off to obtain good quality western blotting images.

4.13. Co-IP. The total proteins in EC109 and EC9706 were harvested, and the supernatants were incubated with 30 μL of protein in A/G agarose (Santa Cruz Biotechnology, USA) and 8 μL of Piezo1 antibody (Abcam, USA) at 4 °C overnight. Precipitated immune complexes were then analyzed by western blotting using antibodies against Piezo1 and p53.

4.14. Tumor Xenografts in Nude Mice. Sixteen female BALB/c nude mice aged 4−6 weeks and weighing 16−22 g were purchased from Vital River, Beijing, China. All mice were housed and maintained at our animal facility under pathogen-free conditions according to institutional guidelines. Animal protocols were reviewed and approved by the animal care and use committee at the Henan Institute of Medical and Pharmaceutical Science. The animal experiments complied with the ARRIVE guidelines and were performed in accordance with the UK Animals Act.

Transfected EC109 cells were resuspended in PBS. BALB/c thymus-free nude mice were subcutaneously administered with a 100 μL cell suspension containing 10^7 cells. The tumor size and body weight of mice were measured using a caliper every 2 days for 23 days. Tumor volume (V) was calculated according to the formula $V = \frac{ab^2}{2}$. The mice were sacrificed by cervical dislocation on day 23, and the tumors were removed and weighed. The body weights and tumor growth rates of the mice were assessed.

4.15. Statistical Analysis. All other results were statistically analyzed using GraphPad Prism 5. Significant differences were analyzed using two-tailed Student's t-test. $p < 0.05$ was considered statistically significant.

■ ASSOCIATED CONTENT

Supporting Information

The Supporting Information is available free of charge at https://pubs.acs.org/doi/10.1021/acsomega.1c00505.

Bax, Caspase3, GAPDH, p53, and Piezo1 specificity primers (Table S1) and all protein primary antibodies and their dilutions (Table S2) (PDF)

■ AUTHOR INFORMATION

Corresponding Authors

Liping Dai − *BGI College & Henan Institute of Medical and Pharmaceutical Sciences, Zhengzhou University, Zhengzhou 450052, China*; Phone: 086-15290808333; Email: lpd@zzu.edu.cn

Liguo Zhang − *BGI College & Henan Institute of Medical and Pharmaceutical Sciences, Zhengzhou University, Zhengzhou 450052, China*; Phone: 086-17839908382; Email: lgzhang@zzu.edu.cn

Authors

Lu Gao − *BGI College & Henan Institute of Medical and Pharmaceutical Sciences, Zhengzhou University, Zhengzhou 450052, China*

Yun Ji − *BGI College & Henan Institute of Medical and Pharmaceutical Sciences, Zhengzhou University, Zhengzhou 450052, China*

Lulu Wang − *BGI College & Henan Institute of Medical and Pharmaceutical Sciences, Zhengzhou University, Zhengzhou 450052, China*

Meixia He − *BGI College & Henan Institute of Medical and Pharmaceutical Sciences, Zhengzhou University, Zhengzhou 450052, China*

Xiaojing Yang − *BGI College & Henan Institute of Medical and Pharmaceutical Sciences, Zhengzhou University, Zhengzhou 450052, China*

Yibing Qiu − *BGI College & Henan Institute of Medical and Pharmaceutical Sciences, Zhengzhou University, Zhengzhou 450052, China*

Xu Sun − *Integrated TCM and Western Medicine Department, Affiliated Cancer Hospital of Zhengzhou University, Zhengzhou 450008, China*

Zhenyu Ji − *BGI College & Henan Institute of Medical and Pharmaceutical Sciences, Zhengzhou University, Zhengzhou 450052, China*

Guanrui Yang − *BGI College & Henan Institute of Medical and Pharmaceutical Sciences, Zhengzhou University, Zhengzhou 450052, China*

Jianying Zhang − *BGI College & Henan Institute of Medical and Pharmaceutical Sciences, Zhengzhou University, Zhengzhou 450052, China*

Shanshan Li − *Pathology Department, First Affiliated Hospital of Zhengzhou University, Zhengzhou University, Zhengzhou 450052, China*

Complete contact information is available at: https://pubs.acs.org/10.1021/acsomega.1c00505

Notes

The authors declare no competing financial interest.

■ ACKNOWLEDGMENTS

The authors would like to acknowledge the support from Henan Key Laboratory for Pharmacology of Liver Diseases and the financial support from the National Natural Science Foundation of China (31600676), Key Scientific Research Projects of Colleges and Universities in Henan Province (21A416011), Medical Science and Technique Project of Henan Province (SBGJ202002104), and the Project of Basic Research Fund of Henan Institute of Medical and Pharmacological Sciences (YYYJK201803).

■ REFERENCES

(1) Bieging, K. T.; Mello, S. S.; Attardi, L. D. Unravelling mechanisms of p53-mediated tumour suppression. *Nat. Rev. Cancer* **2014**, *14*, 359−370.

(2) Butcher, D. T.; Alliston, T.; Weaver, V. M. A tense situation: forcing tumour progression. *Nat. Rev. Cancer* **2009**, *9*, 108−122.

(3) Chai, D. M.; Qin, Y. Z.; Wu, S. W.; Ma, L.; Tan, Y. Y.; Yong, X.; Wang, X. L.; Wang, Z. P.; Tao, Y. S. WISP2 exhibits its potential antitumor activity via targeting ERK and E-cadherin pathways in esophageal cancer cells. *J. Exp. Clin. Cancer Res.* **2019**, *38*, 102.

(4) Chen, J. The Cell-Cycle Arrest and Apoptotic Functions of p53 in Tumor Initiation and Progression. *Cold Spring Harb. Perspect Med.* **2016**, *6*, a026104.

(5) Chen, X.; Wanggou, S.; Bodalia, A.; Zhu, M.; Dong, W.; Fan, J. J.; Yin, W. C.; Min, H. K.; Hu, M.; Draghici, D.; et al. A Feedforward Mechanism Mediated by Mechanosensitive Ion Channel PIEZO1 and Tissue Mechanics Promotes Glioma Aggression. *Neuron* **2018**, *100*, 799−815.

(6) Cinar, E.; Zhou, S.; DeCourcey, J.; Wang, Y.; Waugh, R. E.; Wan, J. Piezo1 regulates mechanotransductive release of ATP from human RBCs. *Proc. Natl. Acad. Sci. U. S. A.* **2015**, *112*, 11783−11788.

(7) Coste, B.; Mathur, J.; Schmidt, M.; Earley, T. J.; Ranade, S.; Petrus, M. J.; Dubin, A. E.; Patapoutian, A. Piezo1 and Piezo2 Are Essential

Components of Distinct Mechanically Activated Cation Channels. *Science* **2010**, *330*, 55−60.
(8) Eisenhoffer, G. T.; Loftus, P. D.; Yoshigi, M.; Otsuna, H.; Chien, C. B.; Morcos, P. A.; Rosenblatt, J. Crowding induces live cell extrusion to maintain homeostatic cell numbers in epithelia. *Nature* **2012**, *484*, 546−549.
(9) Ferlay, J.; Soerjomataram, I.; Dikshit, R.; Eser, S.; Mathers, C.; Rebelo, M.; Parkin, D. M.; Forman, D.; Bray, F. Cancer incidence and mortality worldwide: sources, methods and major patterns in GLOBOCAN 2012. *Int. J. Cancer* **2015**, *136*, E359−E386.
(10) Ghadirian, P.; Ekoé, J. M.; Thouez, J. P. Food habits and esophageal cancer: An overview. *Cancer Detect. Prev.* **1992**, *16*, 163−168.
(11) Global Burden of Disease Cancer C; Fitzmaurice, C.; Dicker, D.; Pain, A.; Hamavid, H.; Moradi-Lakeh, M.; MacIntyre, M. F.; Allen, C.; Hansen, G.; Woodbrook, R.; et al. The Global Burden of Cancer 2013. *JAMA Oncol.* **2015**, *1*, 505−527.
(12) Gudipaty, S. A.; Lindblom, J.; Loftus, P. D.; Redd, M. J.; Edes, K.; Davey, C. F.; Krishnegowda, V.; Rosenblatt, J. Mechanical stretch triggers rapid epithelial cell division through Piezo1. *Nature* **2017**, *543*, 118−121.
(13) Han, Y.; Liu, C.; Zhang, D. F.; Men, H. C.; Huo, L. F.; Geng, Q. W.; Wang, S. N.; Gao, Y. T.; Zhang, W.; Zhang, Y. J.; et al. Mechanosensitive ion channel Piezo1 promotes prostate cancer development through the activation of the Akt/mTOR pathway and acceleration of cell cycle. *Int. J. Oncol.* **2019**, *55*, 629−644.
(14) Harris, S. L.; Levine, A. J. The p53 pathway: positive and negative feedback loops. *Oncogene* **2005**, *24*, 2899−2908.
(15) Hung, W. C.; Yang, J. R.; Yankaskas, C. L.; Wong, B. S.; Wu, P. H.; Pardo-Pastor, C.; Serra, S. A.; Chiang, M. J.; Gu, Z.; Wirtz, D.; et al. Confinement Sensing and Signal Optimization via Piezo1/PKA and Myosin II Pathways. *Cell Rep.* **2016**, *15*, 1430−1441.
(16) Ibiebele, T.; Taylor, A.; Whiteman, D.; van der Pols, J. Eating habits and risk of esophageal cancers: A population-based case-control study. *Cancer Causes Control* **2010**, *21*, 1475−1484.
(17) Islami, F.; Pourshams, A.; Nasrollahzadeh, D.; Kamangar, F.; Fahimi, S.; Shakeri, R.; Abedi-Ardekani, B.; Merat, S.; Vahedi, H.; Semnani, S.; et al. Tea drinking habits and oesophageal cancer in a high risk area in northern Iran: population based case-control study. *BMJ* **2009**, *338*, b929−b929.
(18) Jiang, L.; Zhao, Y. D.; Chen, W. X. The Function of the Novel Mechanical Activated Ion Channel Piezo1 in the Human Osteosarcoma Cells. *Med. Sci. Monit.* **2017**, *23*, 5070−5082.
(19) Kim, S. E.; Coste, B.; Chadha, A.; Cook, B.; Patapoutian, A. The role of Drosophila Piezo in mechanical nociception. *Nature* **2012**, *483*, 209−212.
(20) Li, C.; Rezania, S.; Kammerer, S.; Sokolowski, A.; Devaney, T.; Gorischek, A.; Jahn, S.; Hackl, H.; Groschner, K.; Windpassinger, C.; et al. Piezo1 forms mechanosensitive ion channels in the human MCF-7 breast cancer cell line. *Sci. Rep.* **2015**, *5*, 8364.
(21) Liu, C. F.; Zhu, Y. Z.; Lou, W.; Shi, X. B.; White, R. D.; Gao, A. Functional P53 Determines Docetaxel Sensitivity in Prostate Cancer Cells. *J. Urology* **2013**, *73*, E400−E427.
(22) Liu, Y.; Zhi, Y.; Song, H.; Zong, M.; Yi, J.; Mao, G.; Chen, L.; Huang, G.; Experimental GHJJo, and Research CC. S1PR1 promotes proliferation and inhibits apoptosis of esophageal squamous cell carcinoma through activating STAT3 pathway. *J. Exp. Clin. Cancer Res.* **2019**, *38*, 1−15.
(23) Murthy, S. E.; Dubin, A. E.; Patapoutian, A. Piezos thrive under pressure: mechanically activated ion channels in health and disease. *Nat. Rev. Mol. Cell Biol.* **2017**, *18*, 771−783.
(24) Nicholson, D. W.; Ali, A.; Thornberry, N. A.; Vaillancourt, J. P.; Ding, C. K.; Gallant, M.; Gareau, Y.; Griffin, P. R.; Labelle, M.; Lazebnik, Y. A.; et al. Identification and inhibition of the ICE/CED-3 protease necessary for mammalian apoptosis. *Nature* **1995**, *376*, 37−43.
(25) Patel, K.; Wakhisi, J.; Mining, S.; Mwangi, A.; Patel, R. Esophageal Cancer, the Topmost Cancer at MTRH in the Rift Valley, Kenya, and Its Potential Risk Factors. *ISRN Oncol.* **2013**, *2013*, 503249.
(26) Pejin, B.; Jovanovic, K.; Mojovic, M.; Savic, A. New and highly potent antitumor natural products from marine-derived fungi: covering the period from 2003 to 2012. *Curr. Top. Med. Chem.* **2013**, *13*, 2745−2766.
(27) Srivastava, M.; Kapil, U.; Chattopadhyaya, T. K.; Shukla, N. K.; Gnanasekaran, N.; Jain, G. L.; Joshi, Y. K.; Nayar, D. Nutritional risk factors in carcinoma esophagus. *Nutr. Res.* **1995**, *15*, 177−185.
(28) Sun, Y.; Li, M.; Liu, G.; Zhang, X.; Zhi, L.; Zhao, J.; Wang, G. The function of Piezo1 in colon cancer metastasis and its potential regulatory mechanism. *J. Cancer Res. Clin. Oncol.* **2020**, *146*, 1139−1152.
(29) Suzuki, T.; Muraki, Y.; Hatano, N.; Suzuki, H.; Muraki, K. PIEZO1 Channel Is a Potential Regulator of Synovial Sarcoma Cell-Viability. *Int. J. Mol. Sci.* **2018**, *19*, 1452.
(30) Träger, M. M.; Dhayat, S. A. Epigenetics of epithelial-to-mesenchymal transition in pancreatic carcinoma. *Int. J. Cancer* **2017**, *141*, 24−32.
(31) Vay, C.; Hosch, S. B.; Stoecklein, N. H.; Klein, C. A.; Vallbohmer, D.; Link, B. C.; Yekebas, E. F.; Izbicki, J. R.; Knoefel, W. T.; Scheunemann, P. Integrin expression in esophageal squamous cell carcinoma: loss of the physiological integrin expression pattern correlates with disease progression. *PLoS One* **2014**, *9*, No. e109026.
(32) Wang, J.-F.; Kan, Q.-B. The insufficient prognostic power of stenosis in patients with esophageal cancer. *Int. J. Clin. Oncol.* **2017**, *22*, 1050−1051.
(33) Wang, K.; Cai, L.-H.; Lan, B.; Fredberg, J. J. Hidden in the mist no more: physical force in cell biology. *Nat. Methods* **2016**, *13*, 124−125.
(34) Weng, C. Y.; Chen, Y.; Wu, Y.; Liu, X.; Mao, H. B.; Fang, X. S.; Li, B. X.; Wang, L. N.; Guan, M. M.; Liu, G. L.; et al. Silencing UBE4B induces nasopharyngeal carcinoma apoptosis through the activation of caspase3 and p53. *Oncotargets Ther.* **2019**, *12*, 2553−2561.
(35) Wu, J.; Lewis, A. H.; Grandl, J. Touch, Tension, and Transduction − The Function and Regulation of Piezo Ion Channels. *Trends Biochem. Sci.* **2017**, *42*, 57−71.
(36) Yu, H.; Mouw, J. K.; Weaver, V. M. Forcing form and function: biomechanical regulation of tumor evolution. *Trends Cell Biol.* **2011**, *21*, 47−56.
(37) Zhang, J. L.; Zhou, Y. H.; Huang, T. T.; Wu, F.; Liu, L. P.; Kwan, J. S. H.; Cheng, A. S. L.; Yu, J.; To, K. F.; Kang, W. PIEZO1 functions as a potential oncogene by promoting cell proliferation and migration in gastric carcinogenesis. *Mol. Carcinog.* **2018**, *57*, 1144−1155.
(38) Zhang, L.; Liu, X.; Gao, L.; Ji, Y.; Wang, L.; Zhang, C.; Dai, L.; Liu, J.; Ji, Z. Activation of Piezo1 by ultrasonic stimulation and its effect on the permeability of human umbilical vein endothelial cells. *Biomed. Pharmacother.* **2020**, *131*, 110796.
(39) Zhang, Y.; Miao, Y.; Shang, M.; Liu, M.; Liu, R.; Pan, E.; Pu, Y.; Yin, L. LincRNA-p21 leads to G1 arrest by p53 pathway in esophageal squamous cell carcinoma. *Cancer Manag. Res.* **2019**, *Volume 11*, 6201−6214.

https://doi.org/10.1021/acsomega.1c00505
ACS Omega 2021, 6, 10196−10206